



# Hominin skeletal part abundances and claims of deliberate disposal of corpses in the Middle Pleistocene

Charles P. Egeland<sup>a,1</sup>, Manuel Domínguez-Rodrigo<sup>b,c</sup>, Travis Rayne Pickering<sup>d,e,f</sup>, Colin G. Menter<sup>g</sup>, and Jason L. Heaton<sup>e,f,h</sup>

<sup>a</sup>Department of Anthropology, The University of North Carolina at Greensboro, Greensboro, NC 27412; <sup>b</sup>Department of Prehistory, Complutense University, 28040 Madrid, Spain; <sup>c</sup>Instituto de Evolución en África, University of Alcalá de Henares, 28010 Madrid, Spain; <sup>d</sup>Department of Anthropology, University of Wisconsin–Madison, Madison, WI 53706; <sup>e</sup>Evolutionary Studies Institute, University of the Witwatersrand, 2050 Johannesburg, South Africa; <sup>f</sup>Plio-Pleistocene Palaeontology Section, Department of Vertebrates, Ditsong National Museum of Natural History (Transvaal Museum), 0001 Pretoria, South Africa; <sup>g</sup>Department of Biology, University of Florence, 50122 Florence, Italy; and <sup>h</sup>Department of Biology, Birmingham–Southern College, Birmingham, AL 35254

Edited by David J. Meltzer, Southern Methodist University, Dallas, TX, and approved March 2, 2018 (received for review November 3, 2017)

**Humans are set apart from other organisms by the realization of their own mortality. Thus, determining the prehistoric emergence of this capacity is of significant interest to understanding the uniqueness of the human animal. Tracing that capacity chronologically is possible through archaeological investigations that focus on physical markers that reflect “mortality salience.” Among these markers is the deliberate and culturally mediated disposal of corpses. Some Neandertal bone assemblages are among the earliest reasonable claims for the deliberate disposal of hominins, but even these are vigorously debated. More dramatic assertions center on the Middle Pleistocene sites of Sima de los Huesos (SH, Spain) and the Dinaledi Chamber (DC, South Africa), where the remains of multiple hominin individuals were found in deep caves, and under reported taphonomic circumstances that seem to discount the possibility that nonhominin actors and processes contributed to their formation. These claims, with significant implications for charting the evolution of the “human condition,” deserve scrutiny. We test these assertions through machine-learning analyses of hominin skeletal part representation in the SH and DC assemblages. Our results indicate that nonanthropogenic agents and abiotic processes cannot yet be ruled out as significant contributors to the ultimate condition of both collections. This finding does not falsify hypotheses of deliberate disposal for the SH and DC corpses, but does indicate that the data also support partially or completely nonanthropogenic formational histories.**

mortality salience | mortuary behavior | taphonomy | skeletal part frequencies | machine learning

**W**hile some species of nonhuman animals seem to recognize death and grieve for dead conspecifics (1), a central aspect of the human condition is our capacity to anticipate our own death, and thus, ponder the significance of mortality across time and space. Mortuary practices, which encompass a diversity of rituals infused with deep cultural meaning (2), are societal manifestations of this “mortality salience” (3). Thus, understanding the prehistoric emergence of this uniquely human capacity is of significant concern to anthropology specifically and to humanity more generally. Some mortuary practices—including, prominently, deliberate disposal of the dead—have the potential to leave archaeological traces. There is a long, ongoing debate over claims that Late Pleistocene Neandertals deliberately disposed of their dead (4–6). Beyond this continuing controversy, two Middle Pleistocene paleoanthropological sites, the Sima de los Huesos (SH; Sierra de Atapuerca, Spain) and the Dinaledi Chamber (DC; Rising Star Cave System, South Africa), are particularly relevant to investigating the antiquity of culturally mediated mortuary behaviors (*SI Appendix*). Both preserve fossil assemblages dominated by hominin remains within the deep

recesses of caves, and both are interpreted as having formed solely (or nearly solely) through the deliberate disposal of corpses by other hominins (7, 8). If that interpretation is correct, the possibility of mortuary ritual—and all that implies for emergent mortality salience in the human lineage—can be traced to at least approximately 300–600 kiloannum (ka).

Various lines of evidence are presented in support of the deliberate disposal hypothesis for the SH and DC samples. Both are nearly exclusively composed of hominin fossils and are claimed to lack (DC) or nearly lack (SH) bone-surface damage indicative of carnivore involvement in their formation. These shared anomalies of the SH and DC assemblages match taphonomic predictions for deliberate disposal of corpses. However, both assemblages also show strong biases in hominin skeletal part representation, including most prominently a paucity of axial bones and long bone epiphyses, which is a pattern not predicted under deliberate disposal hypotheses. Given the extraordinary human behavioral claims associated with the SH and DC, these discontinuities demand scrutiny.

Machine learning is an increasingly popular set of methods that permits computers to identify patterns within complex, multivariate datasets with statistical “learning” algorithms (9).

## Significance

**Awareness of self-mortality is a uniquely human capacity. Ritualistic treatment of corpses reflects this realization. Two large assemblages of fossil human bones from Spain (Sima de los Huesos, SH) and South Africa (Dinaledi Chamber, DC) are offered as the earliest evidence for mortuary behavior. This interpretation implies that humans had developed a sense of mortal transience by ~600,000 to 300,000 years ago. Machine-learning statistical analyses of the skeletal part representation data upon which hypotheses of deliberate disposal of corpses at SH and DC are based fail to falsify—but also do not provide unequivocal support for—those hypotheses. We thus argue that it is premature to assert that SH and DC shed particular light on the development of the “human condition.”**

Author contributions: C.P.E., M.D.-R., T.R.P., C.G.M., and J.L.H. designed research; C.P.E., M.D.-R., T.R.P., C.G.M., and J.L.H. performed research; C.P.E., M.D.-R., T.R.P., and J.L.H. analyzed data; and C.P.E., M.D.-R., T.R.P., C.G.M., and J.L.H. wrote the paper.

The authors declare no conflict of interest.

This article is a PNAS Direct Submission.

Published under the PNAS license.

<sup>1</sup>To whom correspondence should be addressed. Email: cpegelan@uncg.edu.

This article contains supporting information online at [www.pnas.org/lookup/suppl/doi:10.1073/pnas.1718678115/-DCSupplemental](http://www.pnas.org/lookup/suppl/doi:10.1073/pnas.1718678115/-DCSupplemental).

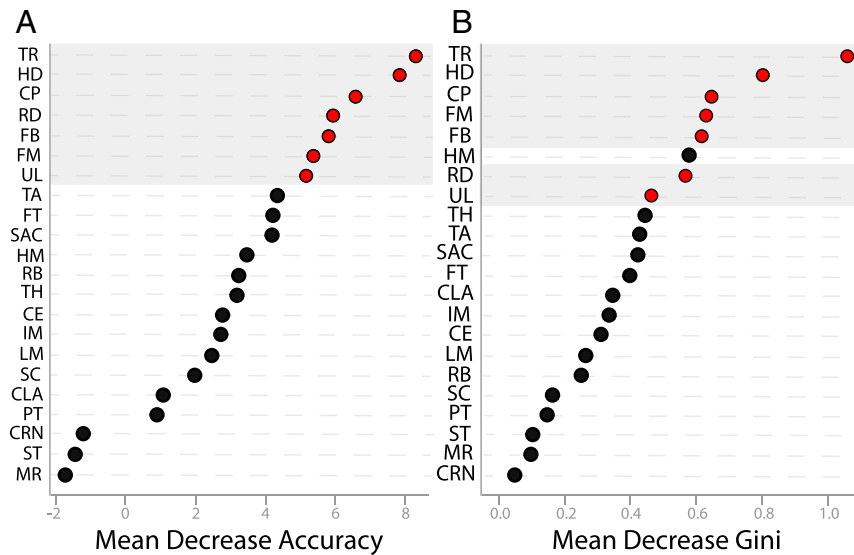


**Fig. 1.** (A) MDA and (B) Gini Index values for 23 skeletal elements or skeletal element groups among the 16 modern and fossil primate assemblages based on a RF analysis. Elements chosen for further analyses (red dots) are highlighted (in gray areas) of both A and B. Abbreviations: CE, cervical; CLA, clavicle; CP, carpals; CRN, cranium; FB, fibula; FM, femur; FT, foot (including metatarsals and pedal phalanges); HD, hand (includes metacarpals and manual phalanges); HM, humerus; IM, innominate; LM, lumbar; MR, mandible; PT, patella; RB, rib; RD, radius; SAC, sacrum; SC, scapula; ST, sternum; TA, tibia; TH, thoracic; TR, tarsals; UL, ulna.

Here, we employ a machine-learning approach that compares hominin skeletal part representation in the SH and DC assemblages to 14 modern and prehistoric accumulations of modern human, archaic human, australopith, and nonhuman primate skeletal remains (Table S1). These 14 assemblages meet the rigorous requirements of our statistical treatments (SI Appendix), having been drawn from a larger sample of 36 published assemblages that we place into the following categories: (i) primary hominin interment (prehistoric); (ii) possible primary hominin interment (prehistoric); (iii) hominin cannibalized/secondary interment (prehistoric); (iv) hominin nonanthropogenically accumulated (prehistoric); (v) undisturbed human corpses (modern); (vi) scavenged human corpses (modern); (vii) leopard-consumed baboon carcasses (modern); and (viii) baboon natural deaths (modern) (detailed definitions of each category are provided in the SI Appendix). While our analyses suggest that anthropogenic activities may have contributed to the formation of the SH and DC hominin assemblages, we believe that claims of Middle Pleistocene corpse disposal nevertheless remain unsettled.

### Results

An exploratory random forest (RF) analysis on all 16 assemblages analyzed here identifies seven skeletal elements or element groups with mean decrease accuracy (MDA) values >5: the tarsals, hand bones (metacarpals and phalanges), carpals, radius, fibula, femur, and ulna (Fig. 1). The discriminatory power of these elements is probably due to characteristics that make them more susceptible to carnivore consumption: small size (tarsals, hand bones, and carpals) or, apart from the femur, low structural density relative to other long bones (radius, fibula, and ulna). Based on the representation of these elements, a three-group model minimizes classification errors and, thus, most parsimoniously divides the assemblages. A *k*-means analysis (using three groups) yields a 2D solution that explains 90.2% of the variance (Fig. 2). Two of the identified groups are associated with high clustering and reduced variance. One comprises undisturbed modern human corpses plus prehistoric primary hominin interments, both of which experienced little or no disturbance and are represented by more-or-less complete skeletons. The other, with the exception of the A.L. 333 *Australopithecus afarensis* sample, includes those assemblages interpreted as hominin cannibalism

and secondary interments. Between these clusters lies a third, more heterogeneous group that consists of the possible prehistoric primary hominin interments, scavenged modern human

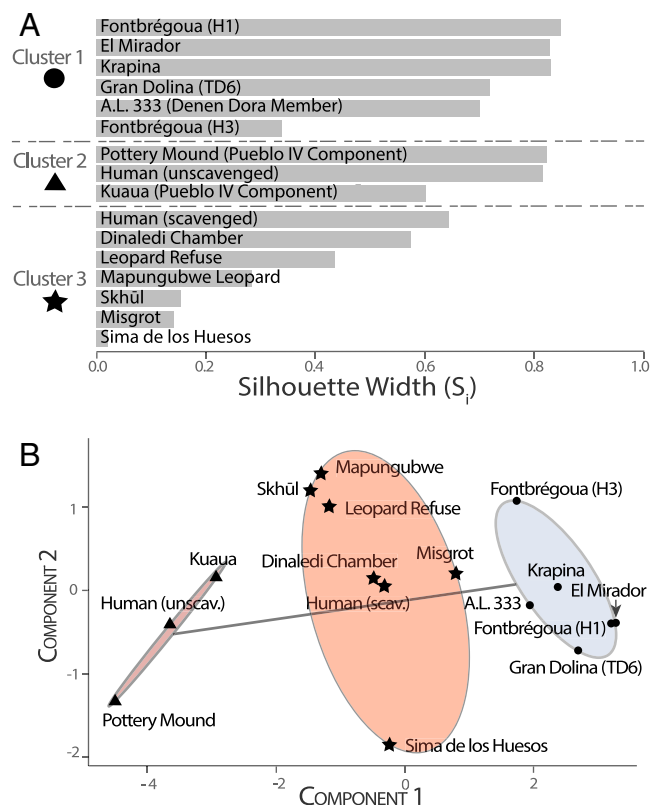


**Fig. 2.** Results of a three-group *k*-means analysis showing (A) a silhouette plot with  $s(i)$  values for each assemblage and (B) a 2D solution illustrating clusters. Average silhouette widths are 0.71 (cluster 1,  $n = 6$ ), 0.75 (cluster 2,  $n = 3$ ), 0.32 (cluster 3,  $n = 7$ ), and 0.55 (all clusters combined). Note: all silhouette values are positive. The two components in B account for 90.26% of the point variability.

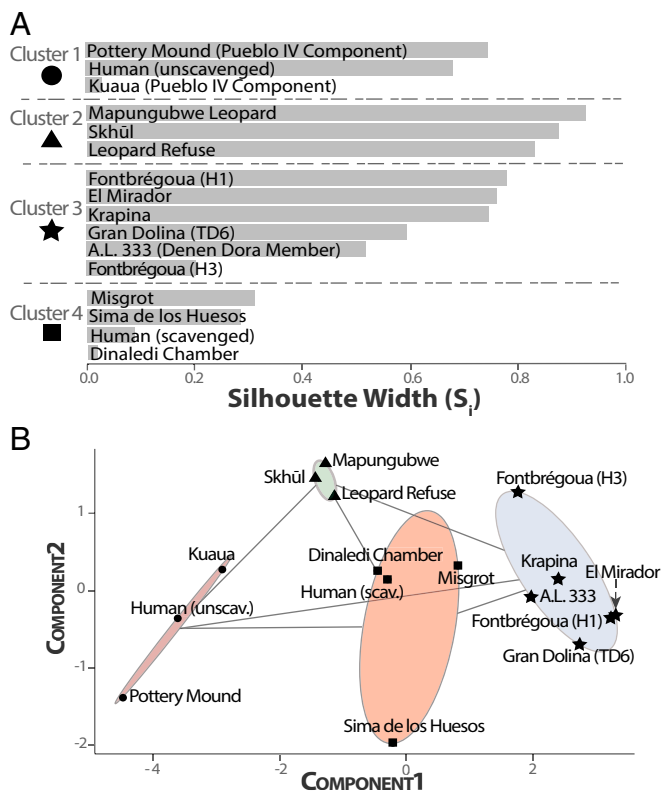


**Fig. 3.** Results of a four-group *k*-means analysis showing (A) a silhouette plot with  $s(i)$  values for each assemblage and (B) a 2D solution illustrating clusters. Average silhouette widths are 0.49 (cluster 1,  $n = 3$ ), 0.88 (cluster 2,  $n = 3$ ), 0.60 (cluster 3,  $n = 6$ ), 0.18 (cluster 4,  $n = 4$ ), and 0.53 (all clusters combined). Like the three-group *k*-means analysis, the two components in B account for 90.26% of the point variability.

corpses, leopard-consumed baboon carcasses, and baboon carcasses accumulated in a cave as the result of natural deaths, each of which experienced some level of disturbance. The SH and DC assemblages occur within this cluster as well. The silhouette plot (Fig. 2) shows SH as the most weakly classified assemblage in this model.

A *k*-means analysis with four groups reinforces the similarities of the SH and DC assemblages with the scavenged modern human corpses and modern cave baboons (Fig. 3), although in this case DC is the most weakly classified assemblage. While the three-group model outperforms the four-group model, we believe that the ability to increase the resolution of the heterogeneous group, which includes the SH and DC collections, with the latter model offsets the reduction in classification strength. Thus, the four-group model is used as the basis for the subsequent machine-learning analyses.

Table 1 summarizes the classification probabilities, based on the abundances of all 23 skeletal elements, for the SH and DC assemblages with each of the machine-learning techniques. In all of the models except for the neural network (NN), the most likely classification of the SH and DC is in the group that includes the modern cave baboons and scavenged modern human corpses. Cohen's  $\kappa$  values indicate that the RF and support vector machine (SVM) analyses are the most powerful (Table 2). The cluster analysis (CA) on principal component analysis (PCA) loading scores using an unsupervised five-group hierarchical classification produces a model that again clusters DC mostly closely with the modern cave baboon assemblage (Fig. 4).

## Discussion

An array of unsupervised multivariate statistical tests (*k*-means, PCA-based CA) and supervised machine learning algorithms (RF, SVM, K-nearest neighbor, decision trees) successfully separate assemblages of undisturbed or minimally disturbed hominin corpses from those that experienced some level of disturbance via cannibalism, secondary interment, and carnivore consumption. These methods also consistently cluster the SH and DC assemblages with the remains of scavenged human corpses, leopard-consumed baboons, and baboons that died naturally within a cave. It is notable, too, that the SH and DC assemblages do not group with El Mirador, which represents a secondary burial.

In other words, the skeletal element abundance data suggest that the SH corpses did not find their way into the cave chamber as complete skeletons and/or that they experienced a substantial level of disturbance after their deposition. While other taphonomic factors may have been at play, we consider the feeding activities of carnivores to be a likely source of this disturbance. Analyses of surface damage on the SH bones reveal that carnivores did, in fact, modify the hominin remains, although the degree of carnivore impact on the final condition of the assemblage is unsettled. To wit, Andrews and Fernández-Jalvo (10) report that >50% of hominin long bone, clavicle, pelvis, sacrum, and rib specimens bear carnivore tooth mark damage. In contrast, Sala et al. (11) find carnivore marks to be much less common, with rates of only 3.7% across the entire skeleton. The damage rates reported by Andrews and Fernández-Jalvo (10) are consistent with—and those of Sala et al. (11) substantially lower than—tooth mark frequencies observed in an assemblage of baboon skeletal remains modified by feeding leopards (12) and in an assemblage of human skeletal remains scavenged by small canids (13), both of which cluster with the SH assemblage based on skeletal element abundances.

It is important to note that even if Sala et al.'s (11) values are closer to representing reality, they still probably underestimate the intensity of carnivore involvement in the formation of the SH assemblage. The prevalence of dry, diagenetic fractures on the SH hominin bones (14) is key here, since such breakage created fragments that did not exist during the corpses' nutritive phases, periods when carnivore damage was presumably inflicted. This disjunction leads to the artificial depression of damage frequencies relative to actualistic controls (see, for example, ref. 15).

We can gauge the effect of this process on the SH mark frequencies through application of a correction method (16). A

**Table 1.** Classification probabilities for the SH and DC assemblages with each of the machine learning techniques

Test	Cluster 1	Cluster 2	Cluster 3	Cluster 4
Neural network				
SH	<b>0.947</b>	0.053	0.000	0.000
DC	<b>0.824</b>	0.176	0.000	0.000
Support vector machine				
SH	0.231	0.198	0.186	<b>0.433</b>
DC	0.109	0.304	0.131	<b>0.511</b>
Decision trees				
SH	0.071	0.036	0.089	<b>0.804</b>
DC	0.071	0.036	0.089	<b>0.804</b>
k-Nearest neighbor				
SH	0.143	0.286	0.143	<b>0.427</b>
DC	0.143	0.286	0.143	<b>0.427</b>
Random forest				
SH	0.191	0.126	0.144	<b>0.543</b>
DC	0.118	0.242	0.161	<b>0.481</b>

Cluster compositions from Fig. 3. Highest probability appears in bold.

**Table 2. Accuracy and Cohen's  $\kappa$  values for each machine learning technique**

Test	Accuracy	Accuracy SD	$\kappa$	$\kappa$ SD
Neural network	0.508	0.180	0.344	0.239
Support vector machine	0.567	0.196	0.422	0.262
Decision trees	0.467	0.127	0.289	0.169
k-Nearest neighbor	0.500	0.000	0.333	0.000
Random forest	0.575	0.149	0.433	0.199

diagenetic break produces, at a minimum, two bone fragments. Thus, the number of diagenetically fractured specimens should be divided by two to reproduce, conservatively, the number of specimens present before diagenetic breakage occurred. This corrected value is then added to the number of specimens broken when bones were fresh (i.e., “green”) to arrive at a more realistic denominator for the calculation of mark frequencies. As an example, consider the 587 long bone (i.e., clavicles, humeri, femora, radii, ulnae, tibiae, fibulae, and metapodials) specimens in Sala et al.'s (14) fracture analysis. Between 62.5% and 90.2% of the specimens identified to each element possess the transverse fracture outlines typically (although not exclusively or uniquely) associated with diagenetic breakage (17). Applying these percentages to the 574 long bone specimens examined for tooth marks (11), 439 are expected to be the result of diagenetic breakage and only 135 (574 – 439) the result of breakage by biotic agents during the nutritive phase. Dividing the estimated frequencies of diagenetically fractured specimens per element by two and adding the resulting value to the estimated frequencies of green broken specimens by element produce a final estimate of the frequency of specimens present before the onset of diagenetic fracture. The corrections using this and other correlates of dry breakage are summarized in Table 3. Across all elements, the revised damage frequencies (7.9–9.2%) are several percentage points higher than the noncorrected value (4.9%) and the damage rates rise significantly for specific elements, like the humerus (from 10.1 to 15.6%–19.1%) and femur (from 18.9 to 30.8%–36.0%). Thus, although carnivore damage on the SH bones may not be severe, it certainly is not negligible.

There is agreement that the modifications on the SH bones were probably inflicted by bears and lions (10, 11). But taphonomic studies of bone remains modified by modern bears reveal patterns of skeletal part representation that differ from that of the SH (18), and modern and prehistoric bear damage to the bones of consumed animals (18–20) diverges from that documented on the SH hominin remains (11). There are similar inconsistencies between what is understood about modern lions as taphonomic agents (21) and what is observed in the SH assemblage (10, 11). The application of a taphotype approach, which identifies taxon-specific patterns of furrowing and tooth-marking (22), may help resolve this issue at some point.

As to the DC assemblage, skeletal part data suggest that, similar to the situation at the SH, hominin corpses did not arrive in the chamber as complete skeletons and/or experienced some postdepositional disturbance (see also ref. 23). Dirks et al. (7) are careful to point out that particular bone fragments are excluded from their preliminary element frequency estimates, which means that the DC skeletal part abundances probably underestimate the number of represented elements to a greater degree than do counting methods that consider all identified fragments. Given the collection procedures imposed by the cramped quarters of the cave chamber, it remains unclear how representative the excavated DC assemblage is of the complete deposited assemblage (24). Nevertheless, the recurrent clustering of the DC assemblage with the disturbed and carnivore-consumed

samples and, in particular, the naturally accumulated bone sample of cave baboons, is intriguing.

To this point, Val (23) questions the conclusion that the DC hominin remains lack carnivore damage (7, 24) and, in so doing, raises what we consider to be legitimate concerns: (i) only about one-third (559 of a total of 1,550) of the recovered hominin specimens were inspected microscopically for surface modifications; and (ii) surface preservation of the DC bones is generally poor, which may obscure or eliminate original surface modifications, including carnivore damage. Given the positive relationship between the size of a bone specimen and the probability of mark appearance on that specimen (25), it is possible that the subset of DC bones subject to analysis, which includes the larger and more complete specimens (7), is that most likely to preserve marks. However, given the uniqueness of the DC sample and the remarkable behavioral claims attached to it, it seems obvious that the entire assemblage should be analyzed carefully for surface modifications. Even more worrisome is that “few [of the DC bone] specimens preserve a pristine surface morphology” (7). Most surface-quality appraisals correspond instead to the types of poorly preserved bones categorized as grade 3 (“[m]ost of bone surface affected by some degree of erosion...general morphology maintained but detail of parts of surface masked by erosive action”) and grade 4 (“[a]ll of bone surface affected by erosive action...general profile maintained and depth of modification not uniform across whole surface”) in McKinley's (26) system.

Moreover, under the variable “surface removal” in Dirks et al.'s (7) supplemental data, 553 of the 559 analyzed specimens (98.9%) score as “outer cortical layers gone.” While this description does not necessarily imply the removal of the entirety of a specimen's cortical layer (24), we think, given the regularity

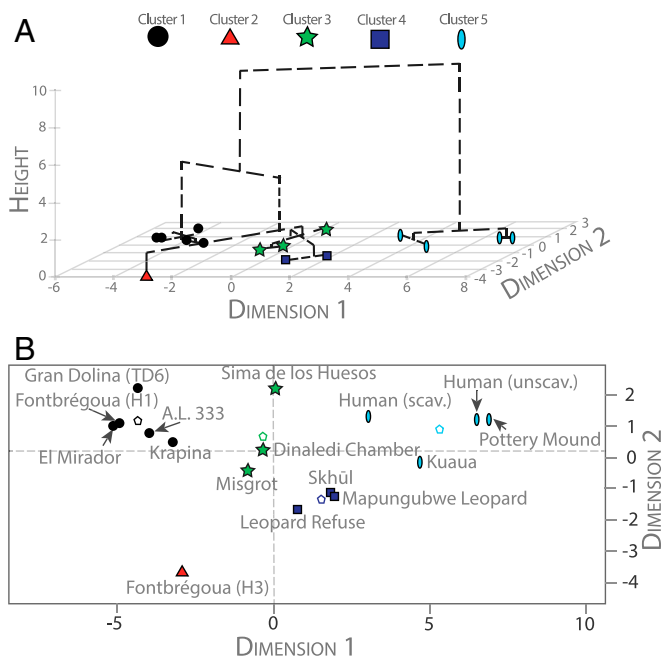


**Fig. 4.** Results of the CA on PCA loading scores using an unsupervised five-group hierarchical classification. The resulting clusters are shown in (A) the hierarchical classification and (B) 2D solution. In A, the height of the dotted lines demonstrate similarity (of the individual sites) within and between each cluster. However, points for Skhul and Mapungubwe Leopard cannot be distinguished (in A) from one another, because of their similarity. In B, pentagon outlines (color labeled) for each cluster display the group's average. Fontbrégoua (H3) is the only site within cluster 2; therefore, no pentagon is shown. The cluster analysis accounts for 76.61% of the sample's variation.

**Table 3. Corrected tooth mark frequencies using correlates of dry breakage for the SH**

Element	%NISP diagenetic NISP	%NISP diagenetic breaks	NISP diagenetic	NISP NISP green	Corrected prediagenetic NISP	Corrected Corrected NISP	NISP TM	Corrected % NISP TM	Uncorrected %NISP TM
<b>Transverse breaks</b>									
CLA	42	0.652	27	15	14	28	0	0.0	0.0
HM	89	0.706	63	26	31	58	9	15.6	10.1
RD	63	0.820	52	11	26	37	1	2.7	1.6
UL	59	0.900	53	6	27	32	1	3.1	1.7
MC	89	0.730	65	24	32	57	1	1.8	1.1
FM	79	0.817	65	14	32	47	15	32.1	18.9
TA	33	0.820	27	6	14	19	1	5.1	3.0
FB		0.902	0	0	0	0			
MT	120	0.725	87	33	44	77	0	0.0	0.0
Total	574		439	135	219	355	28	7.9	4.9
<b>Right-angled breaks</b>									
CLA	42	1.000	42	0	21	21	0	0.0	0.0
HM	89	0.846	75	14	38	51	9	17.5	10.1
RD	63	0.965	61	2	30	33	1	3.1	1.6
UL	59	0.982	58	1	29	30	1	3.3	1.7
MC	89	0.667	59	30	30	59	1	1.7	1.1
FM	79	0.767	61	18	30	49	15	30.8	18.9
TA	33	0.795	26	7	13	20	1	5.0	3.0
FB		0.928	0	0	0	0			
MT	120	0.721	87	33	43	77	0	0.0	0.0
Total	574		469	135	219	340	28	8.2	4.9
<b>Jagged breaks</b>									
CLA	42	1	42	0	21	21	0	0.0	0.0
HM	89	0.939	84	5	42	47	9	19.1	10.1
RD	63	1	63	0	32	32	1	3.2	1.6
UL	59	0.964	57	2	28	31	1	3.3	1.7
MC	89	0.875	78	11	39	50	1	2.0	1.1
FM	79	0.946	75	4	37	42	15	36.0	18.9
TA	33	0.967	32	1	16	17	1	5.9	3.0
FB		0.969	0	0	0	0			
MT	120	0.933	112	8	56	64	0	0.0	0.0
Total	574		542	135	219	303	28	9.2	4.9

NISP, number of identified specimens; TM, tooth-marked. Breakage frequencies from Sala et al. (table 1 in ref. 11). Element NISPs, NISP TM, and Uncorrected %NISP TM from Sala et al. (table 1 in ref. 11). Tooth mark frequencies for fibulae are not reported. NISP Diagenetic = NISP × %NISP Diagenetic Breakage; NISP Green = NISP – NISP Diagenetic; Corrected Prediagenetic NISP = NISP Diagenetic<sup>2</sup>; Corrected NISP = NISP Green + Corrected Prediagenetic NISP; Corrected %NISP TM = NISP TM/Corrected NISP. See Fig. 1 for skeletal element abbreviations.

and severity of surface degradation within the DC assemblage, the possibility that evidence of carnivore involvement was eliminated, or at least rendered inconspicuous or unclear, should not yet be dismissed. Even in the absence of direct carnivore involvement, our machine-learning results for an assemblage composed of baboon remains accumulated by natural die-off in a cave demonstrate that an assemblage composed almost exclusively of a single, large-bodied primate with skeletal patterning like that seen in the DC need not necessarily require deliberate disposal by conspecifics.

## Conclusions

The SH and DC preserve two of the most extraordinary collections of hominin remains in the world. Apart from the contributions of each to studies of hominin taxonomy, variability, and functional morphology (27–30), clarifying the depositional history of each is potentially significant for understanding the evolution of hominin mortuary behavior and, in turn, for charting the development of mortality salience, a uniquely human capacity that sets us apart from other organisms.

Our analysis suggests that the interlinked, latter set of goals is not yet fulfilled. Representation of hominin skeletal parts in both assemblages does not correspond with primary human interments composed of complete skeletons. Rather, both the SH and DC

bone samples cluster with comparative assemblages that experienced moderate to high levels of disturbance, whether through carnivore activities, abiotic postdepositional processes, or hominin-directed butchery and secondary interment. We stress that the results presented here do not refute outright a hominin origin for the SH and DC assemblages, but we do contend that the data also support partially or completely nonanthropogenic formational histories. In a more comprehensive review of Paleolithic mortuary practices, Stiner (6), who is skeptical that the DC reflects deliberate disposal but accepts the SH as largely anthropogenic, argues that neither assemblage occurs in a context that convincingly demonstrates evidence for the long-term, proactive mourning that characterizes symbolic rituals among later humans. In light of these results and considerations, we argue that neither the SH nor DC currently qualifies as unequivocal evidence for emergent mortality salience in the human lineage.

**ACKNOWLEDGMENTS.** We thank the editor and two anonymous referees for their thoughtful and constructive critiques; Charné Nel, for generously sharing data on the Misgrot tooth mark frequencies; and R. Balzac for inspiration and support. M.D.-R. acknowledges the Ministry of Economy and Competitiveness for its support of the HAR2013-45246-C3-1-P Project. T.R.P.'s research was funded by a Kellet Mid-Career Award from the University of Wisconsin–Madison. Research at Misgrot was funded by the Palaeontological Scientific Trust.

1. King BJ (2013) *How Animals Grieve* (Univ of Chicago Press, Chicago).
2. Metcalf P, Huntington R (1991) *Celebrations of Death: The Anthropology of Mortuary Ritual* (Cambridge Univ Press, Cambridge, UK).
3. Greenberg J, Pyszczynski T, Solomon S (1986) The causes and consequences of a need for self-esteem: A terror management theory. *Public Self and Private Self*, ed Baumeister RF (Springer, New York), pp 189–212.
4. Gargett RH (1999) Middle Palaeolithic burial is not a dead issue: The view from Qafzeh, Saint-Césaire, Kebara, Amud, and Dederiyeh. *J Hum Evol* 37:27–90.
5. Pettitt PB (2011) *The Palaeolithic Origins of Human Burial* (Routledge, Abingdon, UK).
6. Stiner MC (2017) Love and death in the Stone Age: What constitutes first evidence of mortuary treatment of the human body? *Biol Theory* 12:248–261.
7. Dirks PHGM, et al. (2015) Geological and taphonomic context for the new hominin species *Homo naledi* from the Dinaledi Chamber, South Africa. *eLife* 4:e09561.
8. Arsuaga JL, et al. (1997) Sima de los Huesos (Sierra de Atapuerca, Spain). The site. *J Hum Evol* 33:109–127.
9. Kuhn M, Johnson K (2013) *Applied Predictive Modeling* (Springer, New York).
10. Andrews P, Fernández Jalvo Y (1997) Surface modifications of the Sima de los Huesos fossil humans. *J Hum Evol* 33:191–217.
11. Sala N, Arsuaga JL, Martínez I, Gracia-Téllez A (2014) Carnivore activity in the Sima de los Huesos (Atapuerca, Spain) hominin sample. *Quat Sci Rev* 97:71–83.
12. Pickering TR, Heaton JL, Zwodski SE, Kuman K (2011) Taphonomy of bones from baboons killed and eaten by wild leopards in Mapungubwe National Park, South Africa. *J Taphon* 9:117–159.
13. Haglund WD, Reay DT, Swindler DR (1988) Tooth mark artifacts and survival of bones in animal scavenged human skeletons. *J Forensic Sci* 33:985–997.
14. Sala N, Arsuaga JL, Martínez I, Gracia-Téllez A (2015) Breakage patterns in Sima de los Huesos (Atapuerca, Spain) hominin sample. *J Archaeol Sci* 55:113–121.
15. Blumenschine RJ (1995) Percussion marks, tooth marks, and experimental determinations of the timing of hominid and carnivore access to long bones at FLK Zinjanthropus, Olduvai Gorge, Tanzania. *J Hum Evol* 29:21–51.
16. Pickering TR, Egeland CP, Domínguez-Rodrigo M, Brain CK, Schnell AG (2008) Testing the “shift in the balance of power” hypothesis at Swartkrans, South Africa: Hominid cave use and subsistence behavior in the Early Pleistocene. *J Anthropol Archaeol* 27: 30–45.
17. Johnson E (1985) Current developments in bone technology. *Adv Archaeol Method Theory* 8:157–235.
18. Arilla M, Rosell J, Blasco R, Domínguez-Rodrigo M, Pickering TR (2014) The “bear” essentials: Actualistic research on *Ursus arctos arctos* in the Spanish Pyrenees and its implications for paleontology and archaeology. *PLoS One* 9:e102457.
19. Sala N, Arsuaga JL (2013) Taphonomic studies with wild brown bears (*Ursus arctos*) in the mountains of northern Spain. *J Archaeol Sci* 40:1389–1396.
20. Pinto AC, Andrews PJ (2004) Scavenging behaviour patterns in cave bears *Ursus spelaeus*. *Rev Paleobiol* 23:845–853.
21. Gidna AO, Kisui B, Mabulla A, Musiba C, Domínguez-Rodrigo M (2014) An ecological neo-taphonomic study of carcass consumption by lions in Tarangire National Park (Tanzania) and its relevance for human evolutionary biology. *Quat Int* 322–323: 167–180.
22. Domínguez-Rodrigo M, et al. (2015) A new methodological approach to the taphonomic study of paleontological and archaeological faunal assemblages: A preliminary case study from Olduvai gorge (Tanzania). *J Archaeol Sci* 59:35–53.
23. Val A (2016) Deliberate body disposal by hominins in the Dinaledi Chamber, Cradle of Humankind, South Africa? *J Hum Evol* 96:145–148.
24. Dirks PHGM, et al. (2016) Comment on “Deliberate body disposal by hominins in the Dinaledi Chamber, Cradle of Humankind, South Africa?”. *J Hum Evol* 96:149–153.
25. Faith JT (2007) Sources of variation in carnivore tooth-mark frequencies in a modern spotted hyena (*Crocuta crocuta*) den assemblage, Amboseli Park, Kenya. *J Archaeol Sci* 34:1601–1609.
26. McKinley JJ (2004) Compiling a skeletal inventory: Disarticulated and co-mingled remains. *Guidelines to the Standards for Recording Human Remains*, eds Brickley M, McKinley JJ (Institute of Field Archaeologists, Reading, UK), pp 14–17.
27. Arsuaga JL, et al. (2014) Neandertal roots: Cranial and chronological evidence from Sima de los Huesos. *Science* 344:1358–1363.
28. Berger LR, Hawks J, Dirks PHGM, Elliott M, Roberts EM (2017) *Homo naledi* and Pleistocene hominin evolution in subequatorial Africa. *eLife* 6:e24234.
29. Berger LR, et al. (2015) *Homo naledi*, a new species of the genus *Homo* from the Dinaledi Chamber, South Africa. *eLife* 4:e09560.
30. Bermúdez de Castro JM, et al. (2004) The Atapuerca sites and their contribution to the knowledge of human evolution in Europe. *Evol Anthropol* 13:25–41.